

---

# LLM-Assisted Alpha-Fairness for 6 GHz Wi-Fi/NR-U Coexistence: An Agentic Orchestrator for Throughput, Energy, and SLA

---

Anonymous Author(s)

Affiliation

Address

email

## Abstract

1        Unlicensed 6 GHz is becoming a primary workhorse for high-capacity access, with  
2        Wi-Fi and 5G NR-U competing for the same channels under listen-before-talk  
3        (LBT) rules. Operating in this regime requires decisions that jointly trade through-  
4        put, energy, and service-level objectives while remaining safe and auditable. We  
5        present an agentic controller that separates *policy* from *execution*. At the start  
6        of each scheduling epoch the agent summarizes telemetry (per-channel busy and  
7        baseline LBT failure; per-user CQI, backlog, latency, battery, priority, and power  
8        mode) and invokes a large language model (LLM) to propose a small set of inter-  
9        pretable knobs: a fairness index  $\alpha$ , per-channel duty-cycle caps for Wi-Fi/NR-U,  
10       and class weights. A deterministic optimizer then enforces feasibility and computes  
11       an  $\alpha$ -fair allocation that internalizes LBT losses and energy cost; malformed or  
12       unsafe policies are clamped and fall back to a rule baseline. In a 6 GHz simulator  
13       with two 160 MHz channels and mixed Wi-Fi/NR-U users, LLM-assisted policies  
14       consistently improve energy efficiency while keeping throughput competitive with a  
15       strong rule baseline. One LLM lowers total energy by 35.3% at modest throughput  
16       loss, and another attains the best overall trade-off, finishing with higher total bits  
17       (+3.5%) and higher bits/J (+12.2%) than the baseline. We release code, per-epoch  
18       logs, and plotting utilities to reproduce all figures and numbers, illustrating how  
19       transparent, policy-level LLM guidance can safely improve wireless coexistence.

## 20    1 Introduction

21       Unlicensed 6 GHz spectrum is rapidly becoming a workhorse for high-capacity wireless access, with  
22       Wi-Fi 6E/7 and 5G NR-U expected to coexist in the same channels Wang et al. [2022]. The resulting  
23       environment is shaped by LBT rules, bursty traffic, heterogeneous device batteries and priorities,  
24       and tight latency targets for interactive and safety-critical applications. Conventional schedulers are  
25       typically crafted around a fixed objective, such as sum-rate maximization or proportional fairness,  
26       and rely on static heuristics to avoid collisions. While effective in specific regimes, these designs  
27       struggle to adapt when operating conditions drift, and they provide limited knobs to navigate the  
28       three-way tension between throughput, energy, and service-level objectives Liu et al. [2025].

29       State-of-the-art solutions for managing spectrum coexistence between technologies like Wi-Fi and  
30       NR-U predominantly fall into two categories: static rule-based schedulers and complex learning-  
31       based systems like deep reinforcement learning (DRL) Kalahe-Wattege and Beltran [2024]Zhang  
32       et al. [2023b]. Rule-based schedulers are reliable and predictable but are fundamentally brittle; they  
33       are designed with fixed priorities, such as maximizing overall throughput, and struggle to dynamically  
34       adapt when network conditions and objectives change Kalahe-Wattege and Beltran [2024]. For  
35       example, they cannot easily pivot to prioritize energy efficiency or meet a specific user’s urgent  
36       latency demand when the network becomes congested . On the other hand, while DRL agents can

37 learn sophisticated policies to manage these trade-offs, they often operate as "black boxes," making  
 38 their decisions difficult to interpret, audit, or trust in a production network Zhang et al. [2023b] .  
 39 Furthermore, DRL systems require extensive, often impractical, online training cycles to converge on  
 40 an effective policy.

41 Our paper solves this critical gap by introducing an agentic controller that separates high-level  
 42 reasoning from low-level execution. It leverages a LLM to interpret the complex, multi-faceted  
 43 network state and propose a simple, human-understandable set of policy "knobs"—such as the fairness  
 44 level and duty-cycle caps Hao et al. [2024] Wang et al. [2024]. This approach avoids the rigidity of  
 45 fixed rules and the opacity of DRL, providing a solution that is simultaneously adaptive, auditable,  
 46 and capable of intelligently balancing the conflicting objectives of throughput, energy efficiency, and  
 47 service level agreements (SLA) on a dynamic, per-epoch basis.

48 At the start of each scheduling epoch, the agent encodes the observable state—per-channel busy  
 49 levels and baseline LBT failure probabilities for both Wi-Fi and NR-U, together with per-user CQI,  
 50 backlog, latency target, battery state, task priority, and power mode—into a compact JSON summary.  
 51 A high-level policy then chooses a small set of interpretable knobs: a fairness index, per-channel duty-  
 52 cycle caps for each stack, and priority weights across traffic classes. This policy can be instantiated  
 53 either as a deterministic rule or as a LLM prompted to reason about energy-aware, latency-aware  
 54 spectrum sharing.

55 We evaluate the agent in a 6 GHz simulator with two 160 MHz channels and mixed Wi-Fi/NR-U  
 56 populations. Across moderate and high offered loads, LLM-assisted policies consistently reduce  
 57 cumulative energy and improve energy efficiency (bits/J) relative to a strong rule baseline, while  
 58 maintaining competitive or superior cumulative throughput. In a representative scenario, one LLM  
 59 variant lowers total energy by more than a third while the other achieves the best overall trade-off,  
 60 finishing with higher total bits and the highest bits/J.

61 The remainder of this paper is structured as follows. In Section II, we detail the system model and  
 62 formulate the multi-objective resource allocation problem. Section III presents the design of the  
 63 LLM-assisted agentic controller. We describe our simulation environment and the baseline rule-based  
 64 scheduler used for comparison in Section IV. In Section V, we present a comprehensive evaluation of  
 65 our proposed system, analyzing its performance across key metrics of network throughput, energy  
 66 efficiency, and SLA satisfaction against the baseline. Finally, we conclude the paper in Section VI.

## 67 2 System Model and Problem Formulation

### 68 2.1 System Model

69 We consider a 6 GHz unlicensed band shared by Wi-Fi and 5G NR-U. Time is slotted into fixed  
 70 scheduling epochs of length  $\Delta$  seconds (default  $\Delta = 0.1$ ), and all control decisions are recomputed  
 71 once per epoch  $t = 1, 2, \dots$ . The system comprises a finite set of channels  $\mathcal{C}$  (two 160 MHz channels in  
 72 the default configuration) and two coexisting technology stacks  $\mathcal{T} = \{\text{Wi-Fi, NR-U}\}$ . Each channel  
 73  $c \in \mathcal{C}$  has bandwidth  $B_c$  and is characterized by exogenous LBT conditions that vary slowly over  
 74 time. Specifically, for each stack  $t \in \mathcal{T}$  and channel  $c$ , we track a sensed busy fraction  $b_{t,c}(t) \in [0, 1]$   
 75 and a baseline LBT failure probability  $f_{t,c}(t) \in [0, 1]$ , both subjected to small random jitter between  
 76 epochs to emulate environmental dynamics. These quantities are taken as inputs to the scheduler and  
 77 are observable before each decision.

78 Users are partitioned by stack,  $\mathcal{U} = \mathcal{U}_{\text{Wi-Fi}} \cup \mathcal{U}_{\text{NR-U}}$ . A user  $i \in \mathcal{U}$  is described at epoch  $t$  by a channel  
 79 quality indicator  $q_i(t) \in \{0, \dots, 15\}$ , a battery state  $B_i(t) \in [0, 1]$ , a queue backlog  $Q_i(t)$  in bits, a  
 80 latency target  $D_i$  in milliseconds, a task priority class  $k_i \in \{\text{emergency, high, normal, bulk}\}$ , and a  
 81 discrete power mode  $p_i \in \{\text{low, med, high}\}$ . New traffic arrivals  $A_i(t)$  are injected into the queue  
 82 each epoch according to a truncated Gaussian process with a configurable mean; the queue dynamics  
 83 obey

$$Q_i(t+1) = \max\{0, Q_i(t) + A_i(t) - S_i(t)\}, \quad (1)$$

84 where  $S_i(t)$  denotes the number of bits served to user  $i$  during epoch  $t$  Wang et al. [2020]. The  
 85 simulation exposes these elements as first-class state variables that are evolved by a lightweight  
 86 environment model prior to each scheduling step.

87 Physical-layer throughput is modeled via a CQI-to-spectral-efficiency mapping. For user  $i$  on channel  
88  $c$ , the spectral efficiency (bits/s/Hz) is

$$s_{i,c}(t) = \text{SE}(q_i(t)) \cdot \eta_{p_i}, \quad (2)$$

89 where  $\text{SE}(\cdot)$  is a standard 16-level table and  $\eta_{p_i}$  scales the efficiency under the user's power mode. If  
90  $\tau_{i,c}(t) \in [0, 1]$  is the airtime fraction allotted to  $i$  on  $c$  during epoch  $t$ , then the pre-LBT raw rate is

$$r_{i,c}(t) = s_{i,c}(t) B_c \tau_{i,c}(t). \quad (3)$$

91 Shared-channel contention and regulatory LBT constraints induce a stack-channel loss that we  
92 capture with a smooth proxy. Let  $\tau_{t,c}(t) = \sum_{i \in \mathcal{U}_t} \tau_{i,c}(t)$  be the aggregate airtime of stack  $t$  on  
93 channel  $c$  in epoch  $t$ . The loss fraction applied uniformly to all users of  $(t, c)$  is

$$\ell_{t,c}(t) = \min\left\{0.95, f_{t,c}(t) + 0.6 \tau_{t,c}(t) b_{t,c}(t) + 0.2 (\tau_{t,c}(t) + b_{t,c}(t) - 1)_+\right\}, \quad (4)$$

94 with  $(x)_+ = \max\{x, 0\}$ . The post-LBT goodput for user  $i$  on  $c$  is then

$$g_{i,c}(t) = r_{i,c}(t) (1 - \ell_{t,c}(t)), \quad S_i(t) = \Delta \sum_{c \in \mathcal{C}} g_{i,c}(t). \quad (5)$$

95 Energy is modeled through a per-bit cost that depends on the power mode and the achieved spectral  
96 efficiency. Writing  $P(p_i)$  for the mode-dependent transmit power and  $e_{i,c}(t) = P(p_i)/s_{i,c}(t)$  for  
97 joules per bit, the per-epoch energy is

$$E_i(t) = \sum_{c \in \mathcal{C}} e_{i,c}(t) S_i(t). \quad (6)$$

98 The above link, loss, and energy models mirror the implementation used by our simulator, where (4)  
99 is realized as a differentiable proxy to capture LBT-driven collisions/backoff at the stack-channel  
100 granularity.

101 Service-level latency is expressed as an instantaneous rate requirement. Given backlog  $Q_i(t)$  and  
102 latency target  $D_i$ , the minimum rate that avoids deadline slippage within epoch  $t$  is

$$\rho_i(t) = \min\left\{\frac{Q_i(t)}{\Delta}, \frac{Q_i(t)}{D_i/1000}\right\}, \quad (7)$$

103 and an SLA hit is registered whenever  $\sum_c g_{i,c}(t) \geq \rho_i(t)$ . The policy layer that precedes optimization  
104 provides three high-level knobs per epoch: a fairness index  $\alpha \in \{0, 1, 2\}$ , per-channel duty-cycle  
105 caps  $u_c^{\text{Wi-Fi}}, u_c^{\text{NR-U}} \in [0, 1]$ , and priority weights  $\{w_k\}_{k \in \{\text{emergency, high, normal, bulk}\}}$ . Caps are constrained  
106 by sensed load through a headroom rule of the form  $u_c^t \leq 1 - \gamma b_{t,c}(t)$  with  $\gamma \in (0, 1)$ , ensuring  
107 that aggregate scheduled airtime remains feasible under exogenous activity. These quantities are  
108 produced either by a deterministic rule or by a LLM from a compact JSON state summary, and are  
109 clamped to safe ranges before optimization.

## 110 2.2 Problem Formulation

111 Let  $x_{i,c}(t) \in \{0, 1\}$  indicate whether user  $i$  is scheduled on channel  $c$  during epoch  $t$ . Each user  
112 is bound to at most one channel per epoch,  $\sum_c x_{i,c}(t) \leq 1$ , and receives a nonnegative airtime  
113  $\tau_{i,c}(t) \in [0, 1]$  that is consistent with the assignment via  $\tau_{i,c}(t) \leq x_{i,c}(t)$ . Per-stack duty caps  
114 provided by the policy enforce

$$\sum_{i \in \mathcal{U}_{\text{Wi-Fi}}} \tau_{i,c}(t) \leq u_c^{\text{Wi-Fi}}, \quad \sum_{i \in \mathcal{U}_{\text{NR-U}}} \tau_{i,c}(t) \leq u_c^{\text{NR-U}}, \quad \forall c \in \mathcal{C}, \quad (8)$$

115 and interact with LBT through (4)–(5). The per-user post-LBT rate in epoch  $t$  is  $x_i(t) = \sum_c g_{i,c}(t)$ ,  
116 and the per-epoch energy is  $E_i(t)$  in (6). A standard weighted  $\alpha$ -fair utility is adopted Wang and  
117 Zhou [2019],

$$U_\alpha(x) = \begin{cases} \log x, & \alpha = 1, \\ \frac{x^{1-\alpha}}{1-\alpha}, & \alpha \neq 1, \end{cases} \quad x > 0, \quad (9)$$

118 and each user  $i$  is endowed with a base weight  $\theta_i = \frac{w_{k_i}}{0.5 + \beta(B_i)}$  that increases with priority and  
 119 penalizes low battery via a monotone function  $\beta(\cdot)$ . The single-epoch allocation problem can then be  
 120 stated as

$$\begin{aligned} \max_{\{x_{i,c}, \tau_{i,c}\}} \quad & \sum_{i \in \mathcal{U}} \theta_i U_\alpha \left( \sum_{c \in \mathcal{C}} g_{i,c}(t) \right) - \lambda \sum_{i \in \mathcal{U}} E_i(t) \\ \text{s.t.} \quad & \text{link and LBT coupling in (3)–(5),} \\ & \text{caps in (8), } \tau_{i,c}(t) \in [0, 1], x_{i,c}(t) \in \{0, 1\}, \sum_c x_{i,c}(t) \leq 1. \end{aligned} \quad (10)$$

121 Here  $\lambda \geq 0$  trades off energy against throughput in the objective; in our implementation the energy  
 122 term is effectively captured by the interaction of (6) with the weights  $\theta_i$  and per-duty utility densities  
 123 used during channel selection, while the reported  $\alpha$ -fair utility remains the primary figure of merit.  
 124 Hard per-epoch latency guarantees may be included as  $\sum_c g_{i,c}(t) \geq \rho_i(t)$  for selected flows, but  
 125 we favor a pragmatic approach in which minimum “urgent” grants are applied procedurally before  
 126 the proportional  $\alpha$ -fair split on the remaining budget—an approach that preserves tractability while  
 127 honoring latency-sensitive traffic.

128 Problem (10) is solved independently at each epoch using policy-provided knobs  $(\alpha, \{u_c^t\}, \{w_k\})$ ,  
 129 yielding the airtime variables  $\{\tau_{i,c}(t)\}$ , post-LBT rates  $\{g_{i,c}(t)\}$ , and per-epoch metrics (throughput,  
 130 energy, and SLA hit rate) that feed back into the next epoch via (1). This separation between a  
 131 high-level, possibly LLM-driven policy and a verifiable optimizer enables safe orchestration: policy  
 132 outputs are clamped to feasible ranges, and the optimizer enforces hard constraints at execution time.

### 133 3 Method: Agent Architecture

134 This work adopts an agentic architecture that separates high-level spectrum *policy* from low-level  
 135 *optimization*. The policy layer proposes a fairness index  $\alpha$ , per-channel duty-cycle caps for Wi-Fi  
 136 and NR-U, and task-class priority weights from observable telemetry; the optimizer then enforces  
 137 feasibility and computes an  $\alpha$ -fair allocation while accounting for LBT losses, energy, and latency.  
 138 The separation ensures that the intelligence responsible for strategic trade-offs is modular and  
 139 replaceable (rule-based or LLM-driven), whereas the executor is verifiable and deterministic. The  
 140 implementation follows this design in a single-epoch loop with environmental evolution between  
 141 epochs.

#### 142 3.1 Telemetry encoding and policy interface

143 At the beginning of each epoch of length  $\Delta$ , the environment exposes a compact JSON state  
 144 containing channel descriptors (bandwidth  $B_c$ , sensed busy  $b_{t,c}$ , and baseline LBT failure  $f_{t,c}$   
 145 for each stack  $t$  on channel  $c$ ) and user descriptors (CQI  $q_i$ , battery level  $B_i$ , backlog  $Q_i$ , latency target  
 146  $D_i$ , task priority  $k_i$ , and power mode  $p_i$ ). The function `build_state_json` produces this state  
 147 and adds lightweight hints such as candidate  $\alpha$  values. A policy consumes this JSON and returns  
 148 three objects: an  $\alpha \in \{0, 1, 2\}$ ; duty caps  $\{u_c^{\text{Wi-Fi}}, u_c^{\text{NR-U}}\}$ ; and priority weights  $\{w_k\}$  for classes  
 149 `emergency/high/normal/bulk`. The project ships two variants of the policy interface: a rule  
 150 baseline that biases caps toward the busier stack while reserving headroom, and an LLM policy  
 151 that emits a JSON policy either via a chat completion in JSON mode or via a Responses API call  
 152 constrained by a JSON Schema; in both cases the returned values are coerced to safe ranges prior to  
 153 optimization.

#### 154 3.2 Safety, feasibility, and fallbacks

155 The fairness index is restricted to  $\{0, 1, 2\}$ ; duty caps are clipped to  $[0, 1]$  and to a busy-aware  
 156 headroom  $u_c^t \leq 1 - \gamma b_{t,c}$  (with  $\gamma \in (0, 1)$  implemented as 0.5 in the code); and priority weights are  
 157 confined to a bounded interval  $[0.1, 10]$ . If the LLM call fails or returns malformed JSON, the system  
 158 falls back to the deterministic rule policy, ensuring that every epoch yields a feasible control. Optional  
 159 textual rationales from the LLM are preserved for auditability but do not affect the optimizer.

### 160 3.3 Epoch solver: two-stage optimization

161 Given the policy knobs, the optimizer solves the epoch using a two-stage scheme tailored to coexis-  
162 tence with shared LBT losses.

163 The first stage assigns each user to one channel by maximizing a *utility density* computed under  
164 a small probe airtime  $\tau_0$ , which approximates the value per unit of duty cycle while internalizing  
165 energy and latency costs. For user  $i$  on channel  $c$ , the pre-loss rate is  $r_{i,c} = s_{i,c} B_c \tau_0$ , where  $s_{i,c}$  is  
166 the CQI- and power-mode-dependent spectral efficiency. The stack-channel loss is modeled by a  
167 smooth proxy:

$$\ell_{t,c} = \min\{0.95, f_{t,c} + 0.6 \tau_{t,c} b_{t,c} + 0.2 (\tau_{t,c} + b_{t,c} - 1)_+\}, \quad (11)$$

168 with  $\tau_{t,c}$  being the aggregate duty of stack  $t$  on channel  $c$ . The probe goodput is  $g_{i,c} = r_{i,c}(1 - \ell_{t_i,c})$ ,  
169 and the corresponding energy consumed during the probe is  $E_{i,c}^{\text{probe}}$ . The assignment score reflects a  
170 direct trade-off between this goodput and the energy cost, defined as:

$$\Phi_{i,c} = \frac{1}{\tau_0} \left( \underbrace{w_{k_i} \cdot \frac{g_{i,c}}{10^6} \cdot w_{\text{lat}}(D_i)}_{\text{Reward: Weighted Goodput (Mbps)}} - \underbrace{\beta(B_i) \cdot E_{i,c}^{\text{probe}}}_{\text{Cost: Battery-Scaled Energy}} \right), \quad (12)$$

171 where  $w_{k_i}$  is the user’s priority weight,  $w_{\text{lat}}(D_i)$  is a multiplier that increases the reward for latency-  
172 sensitive users (e.g., those with  $D_i \leq 50$  ms), and  $\beta(B_i)$  is a penalty factor that increases as battery  
173 level  $B_i$  decreases. The channel with the maximal score  $\Phi_{i,c}$  is chosen for user  $i$ . This stage has  
174 complexity  $O(|\mathcal{U}| |\mathcal{C}|)$  and captures the primary cross-channel trade-offs.

175 The second stage performs within-channel allocation under the duty caps provided by the policy. For  
176 each channel and stack, the available duty budget  $\leq u_c^t$  is split in two passes. A first pass grants *urgent*  
177 *minimums* to latency-critical or high-priority users, allocating the minimal duty required to meet their  
178 instantaneous rate requirement  $\rho_i = \min\{Q_i/\Delta, Q_i/(D_i/1000)\}$ . A second pass distributes the  
179 residual budget via a weighted  $\alpha$ -fair rule, where user  $i$  receives a portion of the airtime proportional  
180 to:

$$\omega_i = \left( \frac{w_{k_i}}{0.5 + \beta(B_i)} \right) \cdot (\text{served}_i + \varepsilon)^{-\alpha}. \quad (13)$$

181 Here,  $\text{served}_i$  is the service a user has already received within the epoch (from the urgent grant) and  
182  $\varepsilon > 0$  is a small constant to ensure stability. After all duties are provisionally assigned, the final  
183 aggregate duties are used to recompute the stack-channel losses  $\ell_{t,c}$ , from which the final per-user  
184 goodput and energy consumption are determined.

### 185 3.4 SLA evaluation, queue update, and logging

186 Following allocation, the achieved per-user rate  $\sum_c g_{i,c}$  is compared against  $\rho_i$  to determine SLA  
187 hits in the current epoch. The served bits are subtracted from backlogs to update  $Q_i$  for the next  
188 epoch, ensuring tight coupling between control and traffic dynamics. In multi-epoch mode, the driver  
189 `run_multi_epoch` evolves channels and baselines with small Gaussian jitters, injects arrivals with a  
190 configurable mean, repeatedly invokes the epoch solver.

### 191 3.5 LLM-Assisted Decision Making

192 At the beginning of each epoch, the agent summarizes the observable telemetry into a compact JSON  
193 state that includes per-channel descriptors (bandwidth, sensed busy fractions, and baseline LBT  
194 failure rates for each stack) and per-user descriptors (CQI, battery level, backlog, latency target,  
195 task priority, and power mode). This serialization, produced by `build_state_json`, is passed  
196 to a large language model that proposes high-level control knobs: a fairness index  $\alpha \in \{0, 1, 2\}$ ,  
197 per-channel duty-cycle caps for Wi-Fi and NR-U, and task-class priority weights. We implement  
198 two invocation modes to ensure robustness: a chat-completions call constrained to JSON output, and  
199 a Responses-API call that enforces a JSON Schema with strict types and bounds. In both modes  
200 the model is prompted as a spectrum policy orchestrator and asked to trade off latency, energy, and  
201 fairness while avoiding per-user micromanagement. The LLM may return brief rationales, which are  
202 logged for audit but are not used downstream in optimization.

203 The raw policy is never executed directly. Instead, `coerce_policy_from_llm` enforces feasibility  
204 and safety by clamping  $\alpha$  to  $\{0, 1, 2\}$ , projecting duty caps to  $[0, 1]$  and to a busy-aware headroom of  
205 the form  $u_c^t \leq 1 - \gamma b_{t,c}$  (with  $\gamma \in (0, 1)$ ), and restricting priority weights to a bounded interval that  
206 prevents extreme allocations. Any parsing failure, schema violation, or out-of-range proposal triggers  
207 a deterministic rule fallback that biases caps toward the empirically busier stack while reserving  
208 headroom, guaranteeing that every epoch yields a valid policy even under LLM faults.

209 Given the sanitized knobs  $(\alpha, \{u_c^t\}_{c,t}, \{w_k\}_k)$ , the optimizer solves the epoch in two stages. First,  
210 it assigns each user to a single channel by maximizing a probe-time utility density that internalizes  
211 post-LBT goodput, energy cost, deadline pressure, and priority/battery weights. Second, within each  
212 channel and stack, it grants minimal duties to satisfy urgent latency targets and then allocates the  
213 remaining budget according to a weighted  $\alpha$ -fair rule. After duties are finalized, stack-channel LBT  
214 losses are realized and per-user goodputs and energies are computed. The selected  $\alpha$  and per-epoch  
215 metrics (throughput, energy, SLA hit rate) are recorded, and the agent advances to the next epoch  
216 with updated queues. This integration makes the LLM responsible only for transparent, high-level  
217 decisions, while a verifiable executor enforces hard constraints at run time.

218 The core of the interaction between the agent and the LLM is a structured JSON object that serves as  
219 the complete state representation provided at the start of each scheduling epoch. The JSON object is  
220 organized into two primary keys: `channels` and `users`. `channels`: An array of objects detailing  
221 the physical state and contention level of each frequency channel. For each channel, we provide  
222 its bandwidth (`bw_mhz`), the measured busy-time contributed by Wi-Fi and NR-U (`busy_wifi`,  
223 `busy_nru`), and the baseline LBT failure probability. `users`: An array of objects representing the  
224 state of each active user. For each user, the prompt specifies their technology (`tech`), channel quality  
225 indicator (`cqi`), data backlog in bits (`backlog_bits`), remaining time to meet their SLA deadline  
226 (`deadline_s`), battery percentage (`battery_pct`), and assigned service priority class (`priority`).

## 227 4 Experimental Setup and Results

### 228 4.1 Experimental Setup

229 We evaluate the agent in a simulated 6 GHz unlicensed band with two 160 MHz channels shared  
230 by Wi-Fi and NR-U. Each experiment spans  $T=100$  scheduling epochs of length  $\Delta=0.1$  s (total  
231 horizon 10 s) Ghosh [2023]. The default user population includes 16 Wi-Fi and 12 NR-U stations  
232 with heterogeneous channel quality indicators (CQI), battery levels, queue backlogs, latency targets,  
233 task priorities, and power modes. Channel descriptors include sensed busy fractions and baseline  
234 LBT failure probabilities for both stacks, all subject to small Gaussian jitter between epochs to  
235 emulate environmental dynamics. Traffic arrivals are injected every epoch as truncated Gaussians,  
236 and queue evolution follows the standard Lindley recursion. The simulator exposes these elements as  
237 first-class state variables (`User`, `Channel`, `Env`) and advances them via `step_env` before each decision;  
238 the single-epoch solver is called from `one_epoch_allocate`, and multi-epoch orchestration from  
239 `run_multi_epoch`. The code also logs per-epoch throughput (served bits), energy (J), SLA hit rate,  
240 and the fairness index  $\alpha$ . The code is available at: <https://github.com/claudwq/LLM-Assisted-Alpha-Fairness-for-6-GHz-Wi-Fi-NR-U-Coexistence.git>  
241

242 The policy layer is either rule-based or LLM-driven. The rule baseline computes per-channel  
243 duty-cycle caps for the two stacks, reserving headroom as a function of sensed busy, and then chooses  
244 the best-throughput  $\alpha \in \{0, 1, 2\}$  each epoch (“benevolent” baseline). The LLM policy sees the same  
245 telemetry as a compact JSON, selects a single  $\alpha$ , per-channel caps, and class weights, and is then  
246 clamped by `coerce_policy_from_llm` for safety before the optimizer is invoked. The optimizer  
247 itself is deterministic: it assigns a single channel per user via a utility-density score that internalizes  
248 post-LBT goodput, energy cost, and deadline pressure, and then performs a within-channel weighted  
249  $\alpha$ -fair split under the cap constraints, realizing LBT loss and energy using the final aggregate duties.  
250 The complete path and data schema are implemented in `llm_spectrum_agent_fairness.py` and  
251 its LLM interface variant.

252 We compare three methods: **RuleBased** (no LLM, benevolent  $\alpha$ ), **GPT4o-Mini** (LLM-assisted  
253 policy), and **GPT5-Mini** (LLM-assisted policy) Zhang et al. [2023a]. All experiments use seed 2025  
254 and the default arrival and jitter settings in the code unless otherwise noted.

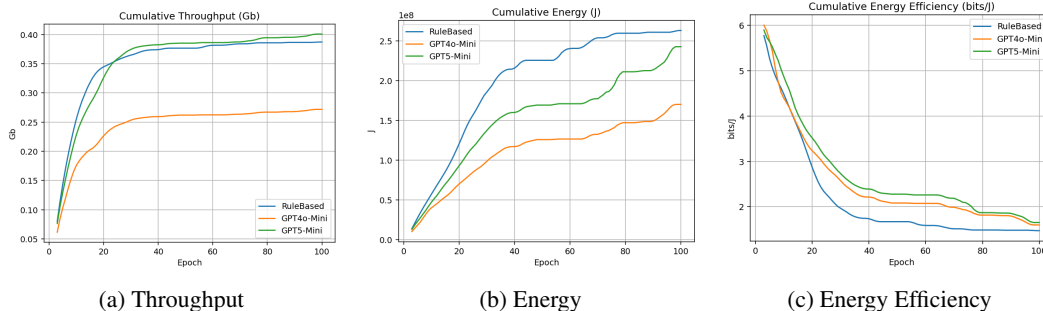


Figure 1: Moderate load (40 Mb/s) results.

## 255 5 Results Analysis

256 We report results for three policies—*RuleBased* (benevolent  $\alpha \in \{0, 1, 2\}$  chosen per epoch), *GPT4o-Mini*,  
 257 *GPT5-Mini*—over  $T=100$  epochs with  $\Delta=0.1$  s. Metrics are computed directly from the  
 258 simulator logs: per-epoch served bits, energy (J), and SLA hit rate; we plot cumulative throughput  
 259 (Gb), cumulative energy (J), and cumulative energy efficiency (bits/J).

### 260 5.1 Moderate Offered Load (40 Mb/s)

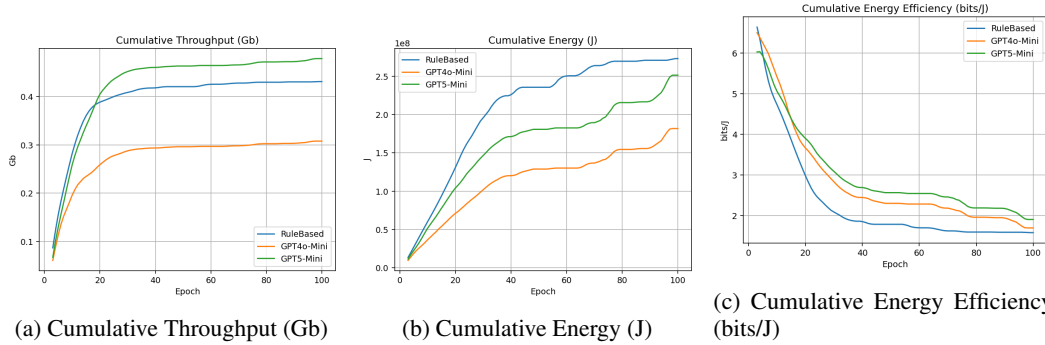
261 Under the moderate arrival rate, cumulative throughput rises rapidly during the first 20–30 epochs as  
 262 the scheduler drains initial backlogs, then transitions to an arrival-limited regime in which curves  
 263 flatten. In this setting, *GPT5-Mini* ultimately surpasses the baseline in total delivered bits while  
 264 spending less energy, whereas *GPT4o-Mini* attains the lowest energy but at the cost of reduced  
 265 throughput. The cumulative energy plots show that *RuleBased* expends the most energy across  
 266 the horizon; this aligns with its tendency to choose  $\alpha=0$  and to push higher duties into collision-  
 267 prone regions. The cumulative energy-efficiency trajectories confirm the advantage of LLM-assisted  
 268 control: both LLM policies maintain higher bits/J than the rule baseline for most of the horizon, with  
 269 *GPT5-Mini* finishing highest. Intuitively, the LLMs propose headroom-aware caps and a fairness  
 270 regime closer to  $\alpha=1$ , which lowers collision losses without starving progress, yielding better energy  
 271 efficiency at comparable or higher cumulative bits.

### 272 5.2 High Offered Load (150 Mb/s)

273 With higher offered traffic the system remains service-limited for longer, and the differences between  
 274 policies become more pronounced. The throughput curves indicate that *GPT5-Mini* sustains the  
 275 fastest cumulative growth and finishes with the highest total bits, while *GPT4o-Mini* again trades  
 276 some throughput for substantial energy savings. Total energy consumption is highest for the rule  
 277 baseline across the entire horizon, reflecting aggressive duty usage that amplifies LBT loss; both  
 278 LLM policies keep cumulative energy lower, and *GPT5-Mini* delivers a favorable balance of bits  
 279 and joules. The energy-efficiency curves mirror these trends: LLM-assisted control dominates the  
 280 baseline throughout most of the run, with *GPT5-Mini* providing the strongest long-horizon bits/J and  
 281 *GPT4o-Mini* offering the best energy containment when energy is the primary objective.

### 282 5.3 Interpretation and Takeaways

283 Across both load regimes, LLM-assisted policies consistently lower cumulative energy and improve  
 284 bits/J relative to the rule baseline, while *GPT5-Mini* achieves the best overall trade-off by pairing  
 285 strong throughput with reduced energy. The qualitative shape of the curves is consistent with the  
 286 agent’s design: LLM-proposed duty caps, combined with a fairness choice nearer to proportional  
 287 fairness, keep the system away from congestion-dominated operating points where additional duty  
 288 yields little goodput but incurs substantial energy. In the moderate-load setting, backlogs drain by  
 289 mid-horizon and per-epoch throughput approaches zero for all methods; the cumulative differences  
 290 observed up to that point therefore reflect more judicious early-phase decisions by the LLM policies.  
 291 In the high-load setting, where the system remains busy, the LLM advantage persists throughout the  
 292 horizon, indicating better long-run operating points under sustained traffic.



(a) Cumulative Throughput (Gb)      (b) Cumulative Energy (J)      (c) Cumulative Energy Efficiency (bits/J)

Figure 2: High offered load (150 Mb/s) over 100 epochs. From left to right: cumulative throughput, cumulative energy, and cumulative energy efficiency.

293 **6 Conclusion**

294 This paper introduced an LLM-assisted spectrum agent for Wi-Fi/NR-U coexistence in the 6 GHz  
 295 band. The core design cleanly separates high-level reasoning from verifiable execution: the policy  
 296 layer—instantiated by a rule or by an LLM—chooses an  $\alpha$ -fairness regime, per-channel duty caps,  
 297 and class weights from compact telemetry, while a deterministic optimizer enforces hard constraints  
 298 and realizes post-LBT goodput and energy. This interface makes the role of the LLM transparent  
 299 and auditable and guarantees safe control through clamping and rule fallback. Across moderate and  
 300 high offered loads, experiments show that LLM-assisted policies reduce cumulative energy and raise  
 301 energy efficiency (bits/J) relative to a benevolent rule baseline, while maintaining competitive or  
 302 superior cumulative throughput. The gains are most pronounced in the early and mid horizon, where  
 303 headroom-aware caps and fairness choices near proportional fairness keep the system away from  
 304 collision-dominated operating points. In a representative 100-epoch scenario, one LLM reduces total  
 305 energy by more than a third, and another achieves the best overall trade-off with higher total bits and  
 306 the highest bits/J among all methods.

307 **References**

308 Monisha Ghosh. Evolution of sharing in 6 ghz. *IEEE Wireless Communications*, 30(5):4–5, 2023.  
 309 doi: 10.1109/MWC.2023.10325444.

310 Nan Hao, Yuangang Li, Kecheng Liu, Songtao Liu, Yingzhou Lu, Bohao Xu, Chenhao Li, Jintai  
 311 Chen, Ling Yue, Tianfan Fu, et al. Artificial intelligence-aided digital twin design: A systematic  
 312 review. 2024.

313 Rasika Nilaweera Kalahe-Wattege and Fernando Beltran. Enhancing throughput for 5g nr-u and wifi  
 314 networks in 6ghz shared-spectrum. In *2024 International Symposium on Networks, Computers  
 315 and Communications (ISNCC)*, pages 1–6, 2024. doi: 10.1109/ISNCC62547.2024.10759054.

316 Sicheng Liu, Qun Wang, Zhuwei Qin, Weishan Zhang, Jingyi Wang, and Xiang Ma. Irs assisted  
 317 decentralized learning for wideband spectrum sensing. *arXiv preprint arXiv:2504.01344*, 2025.

318 Qun Wang and Fuhui Zhou. Fair resource allocation in an mec-enabled ultra-dense iot network with  
 319 noma. In *2019 IEEE International Conference on Communications Workshops (ICC Workshops)*,  
 320 pages 1–6, 2019. doi: 10.1109/ICCW.2019.8757173.

321 Qun Wang, Le Thanh Tan, Rose Qingyang Hu, and Yi Qian. Hierarchical energy-efficient mobile-  
 322 edge computing in iot networks. *IEEE Internet of Things Journal*, 7(12):11626–11639, 2020. doi:  
 323 10.1109/JIOT.2020.3000193.

324 Qun Wang, Haijian Sun, Rose Qingyang Hu, and Arupjyoti Bhuyan. When machine learning  
 325 meets spectrum sharing security: Methodologies and challenges. *IEEE Open Journal of the  
 326 Communications Society*, 3:176–208, 2022. doi: 10.1109/OJCOMS.2022.3146364.

327 Yue Wang, Tianfan Fu, Yinlong Xu, Zihan Ma, Hongxia Xu, Bang Du, Yingzhou Lu, Honghao Gao,  
 328 Jian Wu, and Jintai Chen. Twin-gpt: Digital twins for clinical trials via large language model. *ACM  
 329 Trans. Multimedia Comput. Commun. Appl.*, July 2024. ISSN 1551-6857. doi: 10.1145/3674838.  
 330 URL <https://doi.org/10.1145/3674838>. Just Accepted.



- 331 Chaoning Zhang, Chenshuang Zhang, Sheng Zheng, Yu Qiao, Chenghao Li, Mengchun Zhang,  
332 Sumit Kumar Dam, Chu Myaet Thwal, Ye Lin Tun, Le Luang Huy, et al. A complete survey on  
333 generative ai (aigc): Is chatgpt from gpt-4 to gpt-5 all you need? *arXiv preprint arXiv:2303.11717*,  
334 2023a.
- 335 Xiang Zhang, Arupjyoti Bhuyan, Sneha Kumar Kasera, and Mingyue Ji. Distributed power allocation  
336 for 6-ghz unlicensed spectrum sharing via multi-agent deep reinforcement learning. In *2023*  
337 *IEEE International Conference on Industrial Technology (ICIT)*, pages 1–6, 2023b. doi: 10.1109/  
338 ICIT58465.2023.10143125.

## 339 **Responsible AI Statement**

340 This work adheres to the NeurIPS Code of Ethics. The agent is explicitly designed so that generative  
341 components never execute free-form actions: the large language model (LLM) proposes only a small  
342 set of interpretable, bounded policy knobs (fairness index  $\alpha$ , per-channel duty caps, and priority  
343 weights) from a compact, non-personal telemetry summary. All proposals are validated against a  
344 JSON schema and then clamped to safety ranges, including busy-aware headroom on duty caps;  
345 malformed or out-of-range outputs trigger a deterministic rule fallback. Execution is handled by  
346 a verifiable optimizer that enforces constraints at run time and records decisions for audit. The  
347 simulator contains no personally identifiable information; it uses synthetic traffic and environment  
348 jitter. Potential negative impacts include unsafe spectrum use, unfair service to specific traffic classes,  
349 or excessive energy consumption if the policy is misconfigured. To mitigate these risks, we (i) restrict  
350 the LLM’s authority to high-level proposals with hard constraints; (ii) log every epoch’s knobs and  
351 outcomes for traceability; (iii) provide conservative defaults and seed control; (iv) discuss limits  
352 of our LBT-loss proxy and fairness settings; and (v) refrain from any real-world transmission or  
353 device control in this study. Any future deployment must include regulatory compliance checks (e.g.,  
354 LBT requirements), site-specific validation, and monitoring for distribution shift, with the rule policy  
355 available as a safe fallback.

## 356 **Reproducibility Statement**

357 We provide an anonymized artifact containing code, configuration files, and scripts to re-  
358 generate every figure and table. The simulator exposes fixed seeds and prints the ex-  
359 act run configuration; the optimizer is deterministic given inputs. For the main results,  
360 we include per-epoch CSV logs (`served_bits`, `energy`, `sla_hit_rate`, `alpha_used`) pro-  
361 duced by `llm_spectrum_agent_fairness.py` in multi-epoch mode, and a plotting script  
362 (`plot_three_runs_overlay.py`) that creates all figures and a summary CSV. The artifact docu-  
363 ments the Python version and library hashes, lists command lines to reproduce the 40 Mb/s and  
364 150 Mb/s experiments, and specifies default hyperparameters (epoch length, number of epochs, user  
365 counts, arrival process, jitter magnitudes, seeds, and model identifiers masked for double-blind  
366 review). Because the LLM only emits bounded numeric knobs and the executor is deterministic,  
367 results are stable across runs with the same seed; for completeness we also report partial cumulatives  
368 (25/50 epochs) and provide the raw CSVs used to render each plot.

## 369 **AI Contribution Disclosure Checklist**

### 370 **AI Contribution Disclosure**

371 This work uses large language models (LLMs) as *policy planners* and as assistants for writing and  
372 code refactoring. Model identities are anonymized as *LLM-A* and *LLM-B* for double-blind review.  
373 The execution engine that applies spectrum decisions is deterministic and constraint-enforcing; it  
374 does not depend on generative outputs beyond a small set of bounded numeric knobs.

375 **Roles across the research lifecycle.** Problem framing, system modeling, and the design of the  
376 policy–optimizer split were led by the authors. LLMs assisted ideation by suggesting alternative  
377 fairness/energy/latency trade-offs and by helping refine prose and notation. Simulator and optimizer  
378 implementations were authored by the researchers; LLMs were used to draft code skeletons, to

379 propose interface shapes (e.g., JSON fields for policy knobs), and to streamline plotting and CSV  
380 post-processing. For spectrum control itself, the LLMs served as policy planners: given a compact  
381 telemetry summary, they proposed a fairness index  $\alpha$ , per-channel duty caps for Wi-Fi/NR-U, and  
382 traffic-class weights. Authors retained authority over safety and feasibility: proposals were parsed  
383 under a strict schema, clamped to allowable ranges, and replaced by a rule policy upon any violation  
384 or parsing failure. Experiments, ablations, and quantitative analysis were specified and verified by  
385 the authors; LLMs assisted with script creation and draft figure captions. The manuscript’s first drafts  
386 for several sections were produced with LLM assistance and then edited for technical accuracy and  
387 clarity by the authors.

388 **Safeguards and limits on AI authority.** Generative models do not issue low-level commands  
389 or modify the executor. Their authority is restricted to high-level, interpretable knobs: a discrete  
390  $\alpha \in \{0, 1, 2\}$ , duty-cycle caps projected to  $[0, 1]$  and further limited by busy-aware headroom  
391  $u_c^t \leq 1 - \gamma b_{t,c}$ , and bounded priority weights. Any malformed JSON, schema mismatch, or out-of-  
392 range value triggers an automatic fallback to a deterministic rule policy. At run time, a verifiable  
393 optimizer enforces constraints, realizes LBT losses from the final aggregate duties, and computes  
394 energy from mode-dependent per-bit costs. The system logs the chosen knobs and resulting metrics  
395 every epoch, ensuring traceability and audit.

396 **Data, privacy, and safety considerations.** All experiments are simulation-based with synthetic  
397 traffic; no personal data are used. The work does not transmit over real radios or control physical  
398 infrastructure. Potential risks include unfair service to certain traffic classes or excessive energy usage  
399 if policy knobs were mis-set; these are mitigated by hard clamping, conservative defaults, per-epoch  
400 logging, and a safe rule fallback. Any future deployment would require regulatory compliance checks  
401 (e.g., LBT rules), site-specific validation, monitoring for distribution shift, and human oversight.

402 **Transparency and artifacts.** We provide an anonymized artifact with source code, prompts, schema  
403 definitions, exact commands, seeds, per-epoch CSV logs, and plotting scripts. All figures and  
404 numbers in the paper are generated programmatically from these logs; LLMs did not fabricate results.  
405 The division of responsibilities between AI systems and humans is thus transparent, auditable, and  
406 reproducible.